# 248-nm Laser Photolysis of $CHBr_3$/O-Atom Mixtures: Kinetic Evidence for UV CO(A) Chemiluminescence in the Reaction of Methylidyne Radicals with Atomic Oxygen

**Ghanshyam L. Vaghjiani**

*ERC, Inc., Air Force Research Laboratory, AFRL/PRSA, 10 E Saturn Blvd, Edwards AFB, California 93524*

*Received: August 24, 2004; In Final Form: November 30, 2004*

The 4th positive and Cameron band emissions from electronically excited CO have been observed for the first time in 248-nm pulsed laser photolysis of a trace amount of $CHBr_3$ vapor in an excess of O atoms. O atoms were produced by dissociation of $N_2O$ (or $O_2$) in a cw-microwave discharge cavity in 2.0 Torr of He at 298 K. The CO emission intensity in these bands showed a quadratic dependence on the laser fluence employed. Temporal profiles of the CO(A) and other excited-state products that formed in the photoproduced precursor + O-atom reactions were measured by recording their time-resolved chemiluminescence in discrete vibronic bands. The CO 4th positive transition ($A^1\Pi$, $v' = 0 \rightarrow X^1\Sigma^+$, $v'' = 2$) near 165.7 nm was monitored in this work to deduce the pseudo-first-order decay kinetics of the CO(A) chemiluminescence in the presence of various added substrates ($CH_4$, NO, $N_2O$, $H_2$, and $O_2$). From this, the second-order rate coefficient values were determined for reactions of these substrates with the photoproduced precursors. The measured reactivity trends suggest that the prominent precursors responsible for the CO(A) chemiluminescence are the methylidyne radicals, CH($X^2\Pi$) and CH($a^4\Sigma^-$), whose production requires the absorption of at least 2 laser photons by the photolysis mixture. The O-atom reactions with brominated precursors (CBr, CHBr, and $CBr_2$), which also form in the photolysis, are shown to play a minor role in the production of the CO(A or a) chemiluminescence. However, the $CBr_2$ + O-atom reaction was identified as a significant source for the 289.9-nm $Br_2$ chemiluminescence that was also observed in this work. The 282.2-nm OH and the 336.2-nm NH chemiluminescences were also monitored to deduce the kinetics of CH($X^2\Pi$) and CH($a^4\Sigma^-$) reactions when excess $O_2$ and NO were present.

## 1. Introduction

Methylidyne (CH) is the simplest hydrocarbon radical possible. Its reactions are of interest for understanding chemistry in a wide variety of gas-phase environments, such as those found in interstellar clouds, Jovian atmospheres, hydrocarbon combustion chambers, and high altitude Space Shuttle plumes. Its reactivity with numerous molecular species is well documented in the literature.[1] However, studies of its reactions with atomic species are less common. Reactions with O atoms are of particular interest here.

| | $\Delta H^o_{298K}$ (kcal mol$^{-1}$) | |
|---|---|---|
| $CH(X^2\Pi) + O(^3P) \rightarrow H(^2S) + CO(X^1\Sigma^+)$ | (−175.9) | (1) |
| $\rightarrow HCO(\tilde{X}^2A')$ | (−191.6) | (2) |
| $\rightarrow C(^3P) + OH(X^2\Pi)$ | (−21.4) | (3) |
| $\rightarrow HCO^+(X^1\Sigma^+) + e^-$ | (−4.6) | (4) |

The enthalpies in reactions 1−4 were derived from the heats of formation of the neutrals from the JPL evaluation[2] and of the ion from the NIST chemistry webbook.[3] The overall bimolecular reaction rate coefficient has been determined to be $(9.5 \pm 1.4) \times 10^{-11}$ cm$^3$ molecule$^{-1}$ s$^{-1}$ at 298 K.[4] Channel 4 is thought to be the principal route for primary chemi-ion formation in hydrocarbon flames, and the formyl ion is believed to be involved in soot production.[5] A branching fraction of 0.0003 at 295 K for channel 4 is deduced from Vinckier's measurement of its reaction rate coefficient of $2.4 \times 10^{-14}$ cm$^3$ molecule$^{-1}$ s$^{-1}$.[6] Using the 2200 K data of Peeters and Vinckier,[7] an activation energy of ∼1.6 kcal mol$^{-1}$ can be derived for channel 4. Production of carbon-atoms via channel 3 has theoretically been predicted to be negligible at room temperature because of the significant reaction barrier.[8] Therefore, channels 1 and 2 are expected to be the principal transformation routes. Lin was able to identify the formation of carbon monoxide in channel 1 through its strong 5-$\mu$m ir-emissions.[9] However, no absolute product yields have been reported for these two channels. Also, thermodynamically it should be possible to form the electronically excited products, CO($a^3\Pi$, $a'^3\Sigma^+$, $d^3\Delta$) and HCO($\tilde{A}^2A''$, $\tilde{B}^2A'$, $\tilde{C}^2A''$), in channels 1 and 2, respectively. There are no previous reports of electronic chemiluminescence measurements for channels 1 and 2. It might be that formation of such excited products is facilitated when vibrationally or electronically excited methylidyne is used, as was recently reported in the related (methylidyne + $O_2$) reaction system.[10] Similarly, CH($a^4\Sigma^-$)[11] and CH($A^2\Delta$, $B^2\Sigma^-$)[12] reactions with O atoms have been shown to enhance chemi-ion formation.

Observations of the CO(A→X) and CO(a→X) chemiluminescence when $CHBr_3$ is photodissociated at 248 nm in excess O atoms are reported in this paper. Trends in the decay kinetics of the CO(A) chemiluminescence in various added substrates show that the principal source strength for the radiation is due to the O-atom reactions with the methylidyne radicals in two

* To whom correspondence should be addressed. Tel: 661 275 5657. Fax: 661 275 6245. E-mail: ghanshyam.vaghjiani@edwards.af.mil.

10.1021/jp046172q CCC: $30.25 
Published on Web 02/18/2005

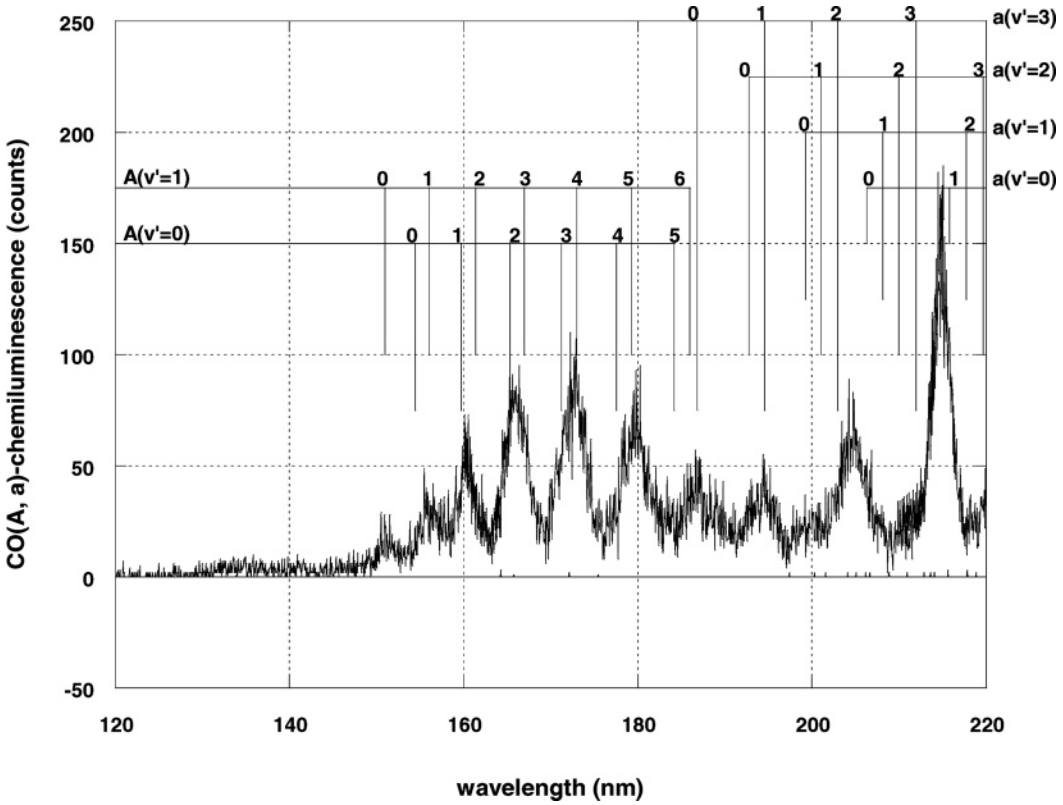


**Figure 1.** Portion of the CO chemiluminescence spectrum obtained 20 $\mu$s immediately after 248-nm laser photolysis of $CHBr_3$ in the presence of an excess of O atoms at 298 K and in 2.0 Torr of He pressure. The O atoms were produced by dissociation of $N_2O$ in a cw-microwave discharge cavity. The background level (in the absence of photolysis) is also shown and on the average is determined to be <0.025 counts for each wavelength data point. The observed vibronic emissions can be assigned to the 4th positive bands, CO(A→X), and the Cameron bands, CO(a→X). The vertical bars illustrate the R(0) and $R_2(0)$ positions of the ($v'$-$v''$) transitions, respectively for the two systems.[21] The data have not been normalized for any variation in the photon detection efficiency of our photomultiplier over this wavelength region.

different electronic states, $CH(a^4\Sigma^-)$ and $CH(X^2\Pi)$. Use of excess $CH_4$ as a selective scavenger for the $CH(X^2\Pi)$ radicals, but not the $CH(a^4\Sigma^-)$ radicals, is made in this work to separately study the CO(A) chemiluminescence contribution in the photolysis from the $CH(a^4\Sigma^-)$ + O reaction. The reactions of brominated radical species such as CBr, CHBr, and $CBr_2$, and C atoms with O atoms, in principle, can also produce CO chemiluminescence but, in the present studies, are of negligible importance. This laboratory work provides evidence for the first time that supports the idea that the interaction of thermospheric O atoms with carbonaceous species such as CH that are present in Space Shuttle plumes could be responsible for part of the far-field ultraviolet emissions observed there.[13]

## 2. Experimental Technique

The pulsed-photolysis/discharge flow-tube apparatus used in this work and the experimental procedures used to record the chemiluminescence data has previously been described in detail elsewhere.[10,14,15] A 1% $N_2O$ or 1% $O_2$ in He mixture was subjected to a cw-microwave discharge in a sidearm cavity to produce O atoms, which were injected upstream into a flow-tube and carried by excess He into the reaction zone to obtain an O-atom concentration of $\sim 1 \times 10^{14}$ molecule $cm^{-3}$ in 2.0 Torr of the buffer gas. Typically $(2-10) \times 10^{12}$ molecule $cm^{-3}$ of $CHBr_3$ was also passed into the reaction zone and subjected to a weakly focusing 248-nm laser beam (5−40 mJ/pulse of energy, operating at 10 Hz) to produce low methylidyne concentrations in the detection volume. Ultraviolet chemiluminescence that ensued from the detection zone was monitored perpendicular to the photolyzing beam by imaging the radiation onto the entrance slits of two different scanning spectrometers positioned opposite to each other. The band-pass of the instruments was 2.0 nm, full-width at half-maximum. The photomultipliers used to detect the radiation were configured for single-photon counting detection, the outputs of which were sent to suitable pulse counting units controlled by microcomputers. Spectral scans of the chemiluminescence were obtained by recording the data starting at 20 $\mu$s after the laser flash and integrating the signal over the next 100 $\mu$s. Typically signals for 20 photolysis flashes were co-added while the spectrometer was continuously scanned very slowly (0.025 nm $s^{-1}$). Time-resolved temporal profiles of the chemiluminescence at selected vibronic band positions in CO(A→X), $Br_2$(D→A), and NH(A→X) when NO was present, and OH(A→X) when $O_2$ was present, were recorded using dwell-time resolutions in the range of 2−10 $\mu$s. A total of 10000 chemiluminescent traces were typically co-added at the computer to improve the signal-to-noise ratio of each of the data sets. The decay kinetics of the chemiluminescence with various added substrates was studied to deduce the corresponding second-order rate coefficient for reaction of the substrate with the precursor radical responsible for generating the excited molecules. The $N_2O$ (99.995%) from Alphagaz was used as received. All other material purities were the same as those stated in previous work.[10]

## 3. Results and Discussion

**3.1. CO(A, a) Chemiluminescence Spectrum.** Figure 1 shows a portion of the chemiluminescence spectrum obtained 20 $\mu$s after the laser photolysis of $CHBr_3$ vapor in excess O atoms produced by the microwave discharge of $N_2O$. The data

are well represented by emissions in the 4th positive and Cameron bands of CO. In this wavelength range, it was confirmed that there was no background chemiluminescence signal from the photolyte/O atom mixture before the laser flash. It was verified that the laser flash did not induce any coincidental long-lived fluorescence in the detection zone of our quartz reactor by recording a background scan in the absence of $CHBr_3$. Scans were also recorded when the microwave discharge power was turned off and the $N_2O$ (or the $O_2$) allowed to flow into the $CHBr_3$ photolysis zone. In this case, the 4th positive CO emission intensity was reduced by ~35 and ~20 times, respectively.[10] This suggests that the O-atom reaction with $CHBr_3$ photolysis product(s) represents the principal source of the observed CO(A) chemiluminescence. The laser fluence dependence of the 165.7-nm CO(A) chemiluminescence was determined to be (1.79 ± 0.20) in the O-atom experiments, which suggests that the relevant photolysis species are formed via 2-photon absorption processes in our experiments.

In the ultraviolet, unit photodissociation of bromoform is thought to proceed principally via Br-atom and $Br_2$ elimination channels.

$$CHBr_3 + h\nu \rightarrow CHBr_2 + Br \quad (5)$$

$$\rightarrow CHBr + Br_2 \quad (6)$$

Bayes and co-workers[16] reported Br-atom primary quantum yields of unity for wavelengths greater than 300 nm and of (0.76 ± 0.03) at 266 nm. Xu and co-workers[17] reported the branching ratio of channels 5 and 6 to be respectively 0.84 and 0.16 at 267 nm and respectively 0.74 and 0.26 at 234 nm. Recently, Zou and co-workers[18] have claimed channel 6 to be negligible for photolysis at 248 nm. The energetics of 1-photon photolysis of bromoform at 248 nm is such that it precludes internally excited $CHBr_2$ and any CHBr that may form from further spontaneously dissociating into smaller fragments. However, both the CHBr and the $CHBr_2$ could subsequently absorb a second 248-nm photon within the same initial laser pulse and dissociate to yield C atoms, CBr, and CH radicals, whereas the $CHBr_2$ in addition could also yield CHBr and $CBr_2$ radicals.[18,19] There are no reports in the literature on the *absolute* yields of the C atoms, CH, CBr, CHBr, and $CBr_2$ radicals in 2-photon 248-nm photolysis of $CHBr_3$ or how the relative product distribution is affected by the laser fluence level. However, evidence that the CHBr yield might be much smaller than CH yield has been discussed by Zou and co-workers[18] and Chang and co-workers.[20] The O-atom reactions with any of these five species could generate the CO(A and/or a) chemiluminescence with the observed quadratic laser fluence dependence as explained below.

Reaction 7, with ground-state reactants, has more than sufficient reaction enthalpy available for the production of CO(A).[2,21] In reactions 8−11, the carbonaceous radicals need to be internally (vibrationally or electronically) excited with energy at least as much as the enthalpies shown below. The experimental heats of formation for CHBr,[22] CBr,[3] and $CBr_2$[23] and those in the JPL evaluation[2] were used in the computations. However, recent ab initio values for the heat of formation of ground-state CHBr[24,25] suggest that reaction 8 may well be exothermic by ~0.1 to ~0.4 kcal $mol^{-1}$.

| | $\Delta H^o_{298K}$ (kcal $mol^{-1}$) | |
|---|---|---|
| $C(^3P) + O(^3P) \rightarrow CO(A^1\Pi)$ | (−71.8) | (7) |
| $CHBr + O(^3P) \rightarrow HBr(X^1\Sigma^+) + CO(A^1\Pi)$ | (+1.3) | (8) |
| $CH + O(^3P) \rightarrow H(^2S) + CO(A^1\Pi)$ | (+9.2) | (9) |
| $CBr + O(^3P) \rightarrow Br(^2P_{3/2}) + CO(A^1\Pi)$ | (+3.8) | (10) |
| $CBr_2 + O(^3P) \rightarrow Br_2(^1\Sigma^+_g) + CO(A^1\Pi)$ | (+29.1) | (11) |

Some measurements of the relative vibrational state distribution within the ground-state for $CH(X^2\Pi)$ formation in $CHBr_3$ photolysis are available;[26,27] however, no such studies have been done for the low-lying first excited-state $CH(a^4\Sigma^-)$ which is also known to form in $CHBr_3$ photolysis.[10,28] The yield of the doublet state relative to the quartet state in CH formation is also not known. State (electronic and/or vibrational) distribution information for bromomethylidyne (CBr), bromomethylene (CHBr), and dibromomethylene ($CBr_2$) is also not known. Previously,[17] Xu and co-workers were unable to confirm $CBr_2$ formation in the multiphoton dissociation of $CHBr_3$ at 234 and 267 nm. This would be consistent with Zou and co-workers'[18] recent findings at 248 nm, who also claimed that the primary photolysis channel 12 is negligible.

$$CHBr_3 + h\nu \rightarrow HBr + CBr_2 \quad (12)$$

To elucidate which of the five carbonaceous species, C atoms, CH*, CBr*, CHBr*, or $CBr_2$* (where * denotes excited species) is the *principal* precursor for CO(A) formation, the decay kinetics of the 165.7-nm CO(A) chemiluminescence was studied in various substrates as described below.

**3.2. CO(A) Chemiluminescence Decay Kinetics.** The precursor, i.e., the photoradical, will react under pseudo-first-order conditions for the case when [precursor] ≪ [O atom]. Since the CO(A) product of the reaction has a very short radiative lifetime (~10 ns), it can be shown that the observed time profile of the associated chemiluminescence in this reaction will follow an exponential decay relationship under our experimental time resolution conditions,[10] with a pseudo-first-order decay coefficient of $k' = k_d + k_O[O] + k_{CHBr_3}[CHBr_3] + \sum(k_{substrate}[substrate])$. $k_d$ is the first-order rate coefficient for diffusion of the precursor out of the detection zone, and $k_O$, $k_{CHBr_3}$, and $k_{substrate}$ are the second-order rate coefficient values for the reaction of the precursor respectively with the O atoms, $CHBr_3$, and the substrates ($CH_4$, NO, $N_2O$, $H_2$, and $O_2$) present in the detection zone. The ● trace of Figure 2 shows a typical 165.7-nm CO(A) chemiluminescence profile observed immediately after $CHBr_3$ is photodissociated in excess O atoms. The trace deviates from the anticipated single exponential form, and there are apparently fast and somewhat slower decay components to it. This behavior has been explained previously to result from multiple and independent precursor reactions that produce the CO(A).[10] Suitable scavenger substrate(s) can be added to the photolysis mixture to rapidly remove one or more of the precursor radicals so as to diminish the production of the CO(A and/or a) chemiluminescence. As in previous work, $CH_4$ was again chosen as the scavenger substrate. An excess of $CH_4$ ($5 \times 10^{15}$ molecule $cm^{-3}$) was added to the photolysis reactor and the CO(A) chemiluminescence recorded in otherwise similar experimental conditions. The ○ trace shows these data where there is an initial rapid drop in the CO(A) chemiluminescent signal followed by what appears to be a single-

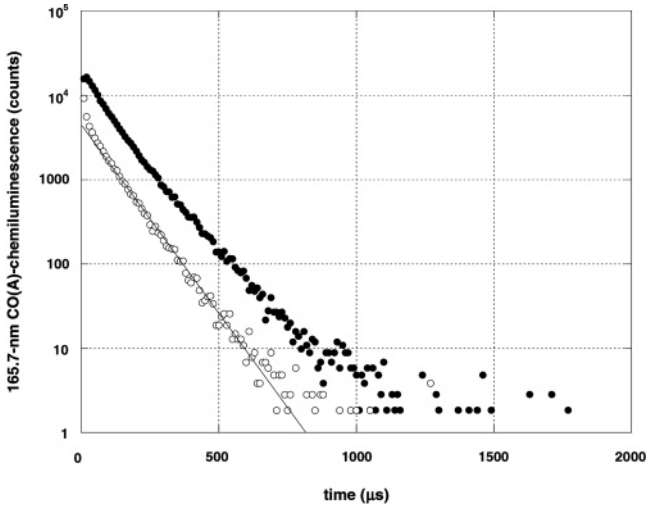


**Figure 2.** Time-resolved 165.7-nm CO(A) chemiluminescence traces observed immediately after 248-nm photolysis of $CHBr_3$ ($5.0 \times 10^{12}$ molecule $cm^{-3}$) in the presence of $O_2$ ($1.1 \times 10^{14}$ molecule $cm^{-3}$) and O atoms ($2.0 \times 10^{13}$ molecule $cm^{-3}$) at 298 K and in 2.0 Torr of He pressure. The O atoms are generated by the microwave discharge of the $O_2$. The ● trace was obtained in the absence of methane and the ○ trace was obtained in the presence of methane ($5.0 \times 10^{15}$ molecule $cm^{-3}$). The time resolution for recording the signal was 10 $\mu$s. A total of 10 000 temporal profiles were co-added to improve the signal-to-noise ratio of the chemiluminescence traces. The pre-laser background was measured to be 0.16 counts and has been removed in the decays shown. The line is an exponential fit (after ~0.1 ms) to the data points of the ○ trace. The magnitude of the slope yields a value for $k'$.

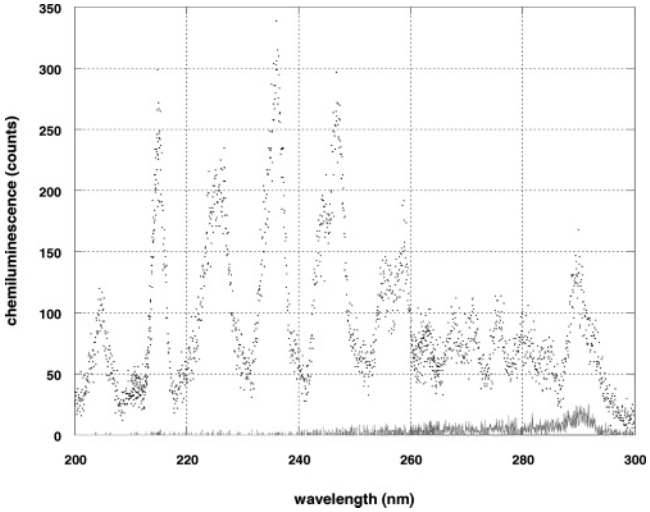


**Figure 3.** Portion of the chemiluminescence spectrum obtained 20 $\mu$s immediately after 248-nm laser photolysis of $CBr_4$ in the presence of an excess of O atoms produced by the microwave discharge of $N_2O$ (● trace). The lower (solid-grey line) trace is the background spectrum obtained in the absence of photolysis with the microwave discharge power on.

exponential decay (for $t > \sim 0.1$ ms). This remaining CO(A) chemiluminescence cannot be due to the O-atom reaction with the doublet state of methylidyne radicals since the added $CH_4$ would rapidly (in less than 10 $\mu$s) consume only the $CH(X^2\Pi)$ but not the $[CH(a^4\Sigma^-)]$.[28] Since the $CH_4$ cannot perturb the [O atom] and does not significantly alter the CO(A) fluorescence yield in the experiment, direct comparison of the areas under the two traces indicates that the ○ trace represents a source strength of ~25% of the total (in the ● trace). The signal strength of the ○ trace was also shown to have a quadratic dependence on the photolysis fluence employed. As discussed latter, the other 75% of the signal strength in the ● trace can be explained by the reaction of O atoms with vibrationally excited, $CH(X^2\Pi, v'' \geq 2)$, radicals.

The decay kinetics of the ○ trace ($t > \sim 0.1$ ms) was then studied in various added substrates. The 298 K values of the second-order rate coefficients, in 2.0 Torr He, were determined to be $k_{N_2O} < 7 \times 10^{-14}$, $k_{NO} = (3.4 \pm 0.5) \times 10^{-11}$, $k_{H_2} < 2 \times 10^{-13}$, and $k_{O_2} = (2.2 \pm 0.3) \times 10^{-11}$ $cm^3$ $molecule^{-1}$ $s^{-1}$, respectively, for the substrates $N_2O$, NO, $H_2$, and $O_2$. On further increasing the $[CH_4]$ in the system, an estimate for $k_{CH_4} < 7 \times 10^{-14}$ $cm^3$ $molecule^{-1}$ $s^{-1}$ was also made. All rate coefficient uncertainties in this work are reported as $1\sigma$ values that include both precision and estimated systematic errors in the rate determinations. From the measured value of $k_{N_2O}$, the (C + O) source reaction 7 is ruled out for this trace as the (C + $N_2O$) reaction rate coefficient is reported to be in the range ($0.8-1.3$) $\times 10^{-11}$ $cm^3$ $molecule^{-1}$ $s^{-1}$.[29-31] (Note that the initial [C] and initial $[CH(a^4\Sigma^-)]$ will remain essentially unperturbed by the $5 \times 10^{15}$ molecule $cm^{-3}$ of $CH_4$.[10,28,29]) Any CHBr* formed in the photolysis will rapidly relax in the 2 Torr of He to the ground-state.[18,32-35] The vibronic lifetimes of electronically excited singlet bromomethylene will be less than a $\mu$s under our experimental conditions.[34,35] Therefore, the reactions of vibrationally and electronically excited singlet bromomethylene, $CHBr(\tilde{A}_{(v'_1,v'_2,v'_3)})$ with O atoms cannot be responsible for the CO(A) chemiluminescence decays of Figure 2. Also, any vibrationally hot $CHBr(\tilde{X}_{(v''_1,v''_2,v''_3)})$ and triplet-bromomethylene, $CHBr(\tilde{a}_{(v'_1,v'_2,v'_3)})$ that are formed will thermalize within ~5 $\mu$s to the ground state.[18,32,33] Therefore, the O-atom reactions of these species cannot explain the traces of Figure 2. Previously, the ground-state (CHBr + $O_2$) reaction rate coefficient has been estimated to be $< 2 \times 10^{-14}$ $cm^3$ $molecule^{-1}$ $s^{-1}$.[36] Hence, the (CHBr + O) reaction 8 cannot be the principal source term for the (open circle) trace and is here considered to be negligible. The remaining curvature (in the range $t > 0.01$ ms and $t < 0.1$ ms) may be an indication that the fast reactions of other brominated excited species, such as $CBr_2$* and CBr*, are partially responsible for the CO(A) signal in this trace.

To ascertain the importance of ($CBr_2$* + O) and (CBr* + O) reactions for the production of CO(A and/or a) chemiluminescence in $CHBr_3$ photolysis, the photolysis of $CBr_4$ was also studied[37] and is briefly reported here. Figure 3 shows part of the chemiluminescence spectrum upper (●) trace recorded 20 $\mu$s after the laser photolysis of $CBr_4$ vapor in excess O atoms produced by the microwave discharge of $N_2O$. The lower (solid-grey line) trace is the background spectrum obtained in the absence of photolysis when the microwave discharge power is on. This feature disappeared when the microwave power was turned off. A similar result was obtained when $O_2$ was dissociated in the microwave cavity. This lower trace shows that there is only a strong feature at ~290 nm (which we have identified to be from $Br_2$* emissions in the (D→A) band, see later discussion) due to the O-atom reaction with a product radical, Y, formed in $CBr_4$ oxidation by O-atom abstraction reactions.[37] Y can only be $CBr_2$ since the ($CBr_3$ + O) reaction will be endothermic for $Br_2$* formation. This 290-nm signal was stronger during photolysis, and its (background subtracted) intensity in the upper trace was shown to have a linear dependence on the laser fluence, whereas the 215-nm Cameron-band feature (and the 165.7-nm 4th positive feature in Figure 4) showed quadratic dependences.[37] This suggests that $CBr_2$ is predominantly produced in $CBr_4$ photolysis through 1-photon absorption and the ($CBr_2$* + O) reaction is *not* the principal source for the CO(A or a) chemiluminescence.[37] Therefore, the major source of CO chemiluminescence could be due to the

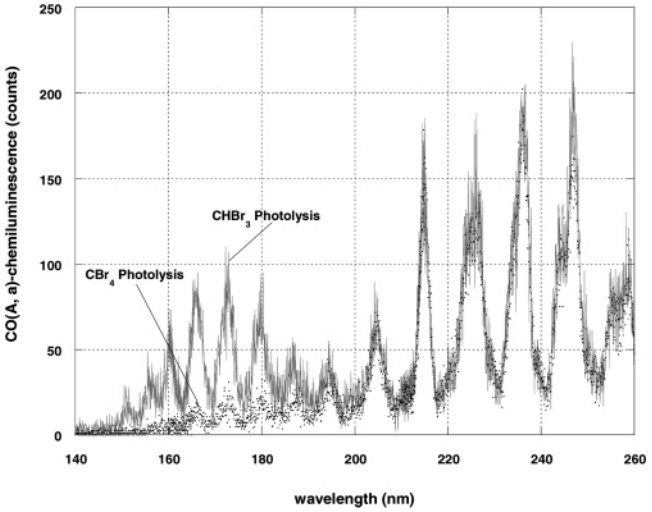


**Figure 4.** Comparison of the CO(A, a) chemiluminescence observed 20 $\mu$s immediately after the photolysis of $4.1 \times 10^{12}$ molecule cm$^{-3}$ of $CBr_4$ (● trace) and $8.8 \times 10^{12}$ molecule cm$^{-3}$ of $CHBr_3$ (solid-grey line) in excess O atoms and 2.0 Torr He. In each case, the O atoms were produced by the microwave discharge of $N_2O$ ($2.5 \times 10^{14}$ molecule cm$^{-3}$) and the laser fluence was kept constant at 10 mJ pulse.

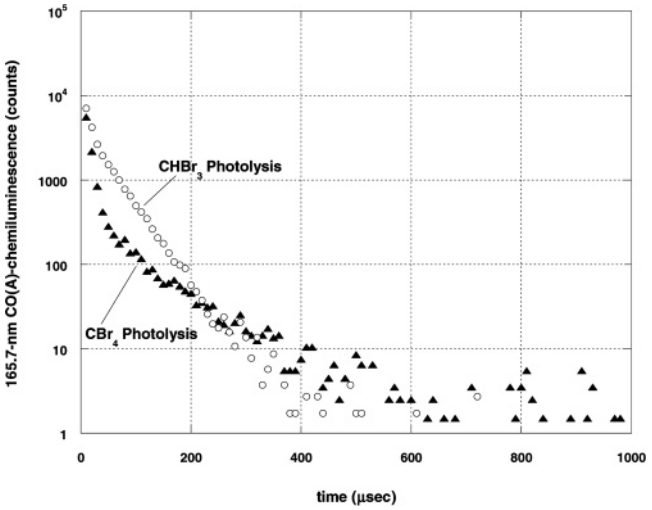


**Figure 5.** Time-resolved 165.7-nm CO(A) chemiluminescence decays observed in the presence of $5 \times 10^{15}$ molecule cm$^{-3}$ of $CH_4$ in the photolysis of $4.2 \times 10^{12}$ of $CBr_4$ (▲ trace) and of $1.0 \times 10^{13}$ of $CHBr_3$ (○ trace) in 2.0 Torr of He. $O_2$ was dissociated in the microwave discharge cavity to produce an O-atom concentration of $3.7 \times 10^{13}$ molecule cm$^{-3}$ in the detection zone.

(CBr* + O) reaction, where the excited bromomethylidyne radical, (CBr* = CBr($X^2\Pi$, $v''$) or = CBr($a^4\Sigma^-$,$v'$)) is produced via 2-photon absorption in $CBr_4$ photolysis. Figure 4 compares the data of $CBr_4$ photolysis with that of $CHBr_3$ photolysis under similar conditions of O atoms and suggests that, in the latter case, the O-atom reaction with a hydrogenated species is more important than that with CBr*. The time-resolved 165.7-nm CO(A) chemiluminescence trace in $CBr_4$ photolysis in excess O atoms also showed nonexponential decay behavior. Figure 5 compares the data when excess $CH_4$ is present in both $CBr_4$ (▲ trace) and $CHBr_3$ (○ trace) for similar O atom/$O_2$ conditions in 2.0 Torr He. The $O_2$ dependence of the ▲ trace for ($t > \sim 0.1$ ms) gave a $k_{O_2}$ value of $(2.5 \pm 0.4) \times 10^{-12}$ cm$^3$ molecule$^{-1}$ s$^{-1}$, which is close to an order-of-magnitude smaller than the value of $(2.2 \pm 0.3) \times 10^{-11}$ cm$^3$ molecule$^{-1}$ s$^{-1}$ obtained for the ○ trace. This demonstrates that the ○ trace of Figures 2 and 5 cannot come from the O-atom reaction with CBr*. The

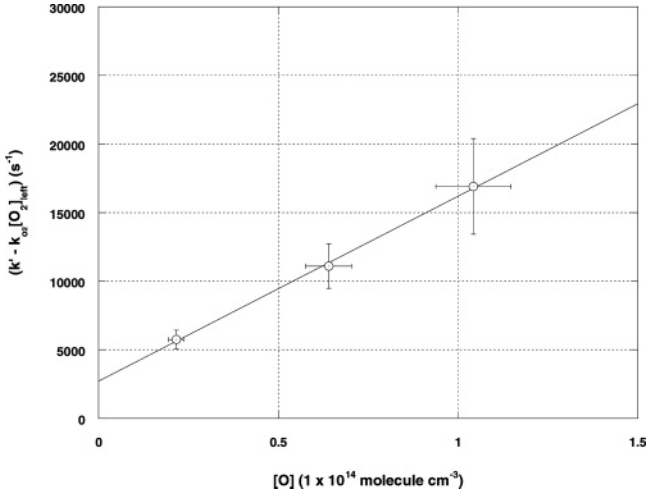


**Figure 6.** Plot of ($k' - k_{O_2}[O_2]_{left}$) as a function of [O] for experiments in which $CHBr_3$ ($7.0 \times 10^{12}$ molecule cm$^{-3}$) was photodissociated in the presence of $CH_4$ ($5.0 \times 10^{15}$ molecule cm$^{-3}$) in 2.0 Torr of He buffer gas at 298 K with a known excess of O atoms and $O_2$. The magnitude of the slope yields a value for the second-order rate coefficient for the (CH($a^4\Sigma^-$) + O) reaction.

above $k_{O_2}$ value in $CBr_4$ photolysis is most likely that for the (CBr($a^4\Sigma^-$) + $O_2$) reaction (it is assumed here that $CH_4$ efficiently relaxes any CBr($X^2\Pi$, $v''$) to the ground-state). No previous measurements are available for comparison, however, its magnitude is similar to that of the ground-state (CBr + $O_2$) reaction.[38,39]

The present $k_{N_2O}$, $k_{NO}$, $k_{H_2}$, $k_{CH_4}$, and $k_{O_2}$ values obtained in the $CHBr_3$ work are in good agreement with previous (CH($a^4\Sigma^-$) + $N_2O$), (CH($a^4\Sigma^-$) + NO), (CH($a^4\Sigma^-$) + $H_2$), (CH($a^4\Sigma^-$) + $CH_4$), and (CH($a^4\Sigma^-$) + $O_2$) reaction rate coefficient measurements, respectively,[10,28] and therefore suggest that the CO(A) chemiluminescence source for the ○ trace of Figure 2 is most likely the (CH($a^4\Sigma^-$) + O($^3$P) → H($^2$S) + CO($A^1\Pi$)) channel, which has a standard reaction enthalpy of $\sim -8.3$ kcal mol$^{-1}$.[21] The energetics of 2-photon production of CH($a^4\Sigma^-$) is such that formation of CO(A) will not be possible for its reaction with the NO but, in principle, should be with the $N_2O$. No overall enhancement in the CO(A) signal was discernible for the range of [$N_2O$]/[O] employed; therefore, the (CH* + O) source term is much stronger than the (CH* + $N_2O$) term in these sets of experiments.

The overall second-order rate coefficient for the (CH($a^4\Sigma^-$) + O($^3$P)) reaction was also determined in this work by varying the [O] by altering the $O_2$ flow going into the microwave discharge cavity. The absolute O-atom density at the detection zone in the experiment was directly determined before hand in a $NO_2$-titration run (O + $NO_2$ → NO + $O_2$), whose end-point was photometrically monitored.[40] Figure 6 shows a plot of the pseudo-first-order decay coefficient of the (CO(A)) ○ trace in Figure 2 that has been corrected for the contribution from the reaction of undissociated $O_2$ (i.e., ($k' - k_{O_2}[O_2]_{left}$)) as a function of [O], where $[O_2]_{left} = ([O_2]_o - [O]/2)$ and $[O_2]_o$ is the number density of molecular oxygen in the detection zone that would be available in the absence of the microwave discharge. The data of Figure 6 is given in Table 1 which also includes the experimentally determined values for $[O_2]_o$, $[O_2]_{left}$, and $k'$. A linear least-squares fit to the data points of the plot yields a value of $k_O = (1.35 \pm 0.47) \times 10^{-10}$ cm$^3$ molecule$^{-1}$ s$^{-1}$ at 298 K in 2 Torr He. The relatively large error in $k_O$ results from the large uncertainty associated in computing ($k' - k_{O_2}[O_2]_{left}$) even though the precision of $k'$ determination is very high in the experiment. There is no previous O-atom rate

**TABLE 1: Experimental Values for $[O_2]_0$, [O], and $[O_2]_{left}$, the Fitted Value of $k'$ from the ○ trace in Figure 2, and Its Corrected Value, ($k' - k_{O_2}[O_2]_{Left}$) Used in Figure 6**

| $[O_2]_0$ ($10^{14}$ molecule cm$^{-3}$) | [O] ($10^{14}$ molecule cm$^{-3}$) | $[O_2]_{left}$ ($10^{14}$ molecule cm$^{-3}$) | $k'$ ($s^{-1}$) | $k' - k_{O_2}[O_2]_{left}$ ($s^{-1}$) |
|---|---|---|---|---|
| $8.55 \pm 0.85$[a] | $1.04 \pm 0.10$ | $8.03 \pm 0.86$ | $33\,768 \pm 338$ | $16\,907 \pm 3488$ |
| $1.67 \pm 0.17$ | $0.22 \pm 0.02$ | $1.55 \pm 0.17$ | $9008 \pm 90$ | $5753 \pm 676$ |
| $4.02 \pm 0.40$ | $0.64 \pm 0.06$ | $3.70 \pm 0.40$ | $18\,881 \pm 188$ | $11\,103 \pm 1613$ |

[a] All uncertainties are $1\sigma$ values.

coefficient measurement for reaction with CH($a^4\Sigma^-$), but the present value is consistent with that for the reaction with CH($X^2\Pi$) previously reported by Messing and co-workers[4] and also by us in this study (see below).

**3.3. OH Chemiluminescence Decay Kinetics.** To confirm the formation of CH($X^2\Pi$) and CH($a^4\Sigma^-$) in $CHBr_3$ photolysis, the OH chemiluminescence was also studied when $O_2$ was added to the system. Figure 7 shows typical chemiluminescence decays observed at 282.2 nm in the absence of O atoms (i.e., microwave discharge power off); the × trace and the △ trace is for $[CH_4] = 0$ and $5.0 \times 10^{15}$ molecule cm$^{-3}$, respectively. When O atoms are present (i.e., microwave discharge power on), the ■ trace and the □ trace were obtained, respectively for $[CH_4] = 0$, and $5.0 \times 10^{15}$ molecule cm$^{-3}$. The × trace represents the time profile of the strong OH(A) (1→0) chemiluminescence predominantly due to the occurrence of the $O_2$ reaction with CH($X^2\Pi$) and to a small extent with CH($a^4\Sigma^-$).[10] Upon adding excess methane, a fast drop in the OH(A) chemiluminescence is observed which would be consistent with the fast removal of any CH($X^2\Pi$) present in the photolyzed mixture.[10,28] The resulting △ trace then represents the time profile of the OH(A) chemiluminescence due to only the (CH($a^4\Sigma^-$) + $O_2$) reaction. By adding various amounts of $N_2O$ to the experiments for these two conditions, the rate coefficient values of $k_{N_2O} = (5.1 \pm 0.9) \times 10-11$ and $<1 \times 10^{-13}$ cm$^3$ molecule$^{-1}$ s$^{-1}$ for $N_2O$ reactions with CH($X^2\Pi$) and CH($a^4\Sigma^-$) were obtained, respectively. Note that these values are similar to those obtained when monitoring the 165.7-nm CO(A) chemiluminescence.

In principle, Cameron band chemiluminescence produced in these $O_2$ reactions would also be detected at this spectrometer setting, e.g., in the weak CO($a^3\Pi$, $v' = 2 \rightarrow X^1\Sigma^+$, $v'' = 8$) band; however, its contribution to the observed signal in the △ trace would be severely suppressed due to efficient CO(a) fluorescence quenching by the excess $CH_4$. The ■ trace shows that the initial time profile is not affected much when O atoms are formed from the $O_2$ (× trace); however, the occurrence of additional chemiluminescence in the system is clearly discernible at long reaction times. Its yield and decay rate are much smaller. This chemiluminescence is neither quenched nor its decay kinetics affected significantly when excess $CH_4$ is added (□ trace). Therefore, an O-atom reaction with a precursor, Y, which predominantly yields an electronically excited species, Z*, other than CO(a) must be responsible for the signal in this time region. However, in the early part (time < ~200 $\mu$s), the ■ trace does get affected by the addition of $CH_4$. The initial portion of this signal is predominantly from OH(A) chemiluminescence which can only come from the methylidyne reactions with the $O_2$. The fast drop (within 20 $\mu$s) in the open square trace is therefore due to the removal of CH($X^2\Pi$) from the system, whereas the phenomenological curved decay in the 20−100 $\mu$s range represents comparable chemiluminescence signals from (CH($a^4\Sigma^-$) + O) and (Y + O) reactions.

A kinetics study of the precursor, Y, was carried out in order to elucidate its identity and that of the electronically excited product, Z*, formed in its reaction with atomic oxygen. For a fixed amount of [O atom] present in the experiments, the ■ traces of Figure 7 were determined at various different $O_2$ concentrations in the range $(2-10) \times 10^{14}$ molecule cm$^{-3}$. Exponential fits were performed in the initial fast decaying part and in the slow decaying part at very long times to extract the values for the pseudo-first-order decay coefficients. Second-order plots of these gave $k_{O_2} = (3.4 \pm 0.6) \times 10^{-11}$ and $< 1 \times 10^{-13}$ cm$^3$ molecule$^{-1}$ s$^{-1}$ for the $O_2$ reactions with CH($X^2\Pi$) and Y, respectively. Then by varying the O-atom concentration by known amounts, an analysis similar to that of Figure 6 was performed for both regions of the trace. This gave $k_O = (1.1 \pm 0.4) \times 10^{-10}$ and $(5.9 \pm 2.1) \times 10^{-11}$ cm$^3$ molecule$^{-1}$ s$^{-1}$ for the O-atom reactions with CH($X^2\Pi$) and Y, respectively. Our (CH($X^2\Pi$) + O) reaction rate coefficient value is in good agreement with the one previous determination[4] and similar to that for the (CH($a^4\Sigma^-$) + O) reaction discussed earlier. The $CH_4$ + Y reaction rate coefficient was also estimated to be $< 7 \times 10^{-14}$ cm$^3$ molecule$^{-1}$ s$^{-1}$. Since ($HCBr_2$ + O)[2] and (HBr + O)[2,22] reactions are both endothermic for the production of electronically excited OH,[21] the slowly decaying chemiluminescence signal in Figure 7 cannot be due to OH(A) emissions. A spectral scan in this wavelength vicinity was therefore recorded as described below in order to determine the identity of the emitter Z*.

**3.4. $Br_2$(D) Chemiluminescence Spectrum and Decay Kinetics.** The spectral scan was recorded in excess methane conditions with sufficiently high $[O_2]$ and at a long delay time after the initial laser flash. The $O_2$ served to increase the rate

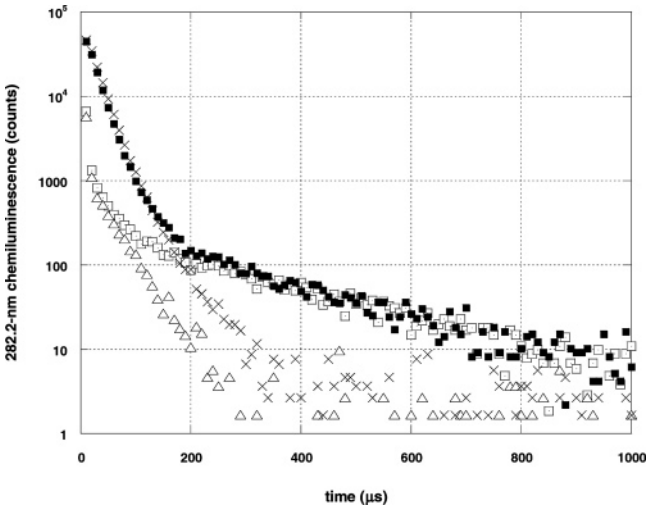


**Figure 7.** Time-resolved 282.2-nm chemiluminescence traces observed immediately after 248-nm photolysis of $CHBr_3$ ($6.0 \times 10^{12}$ molecule cm$^{-3}$) at 298 K in He (2.0 Torr). The × trace is obtained with $O_2$ ($8.8 \times 10^{14}$ molecule cm$^{-3}$) present but in the absence of methane, whereas the △ trace is obtained for the same amount of $O_2$ but with methane ($5.0 \times 10^{15}$ molecule cm$^{-3}$) also present. The □ trace is obtained when O atoms ($5.0 \times 10^{13}$ molecule cm$^{-3}$) are present in the apparatus with both $O_2$ and methane also present, and the ■ trace is obtained with the same amounts of O atoms and $O_2$ present but in the absence of methane. The time resolution for recording the signal was 10 $\mu$s. A total of 10 000 temporal profiles were co-added to improve the signal-to-noise ratio of the chemiluminescence traces.

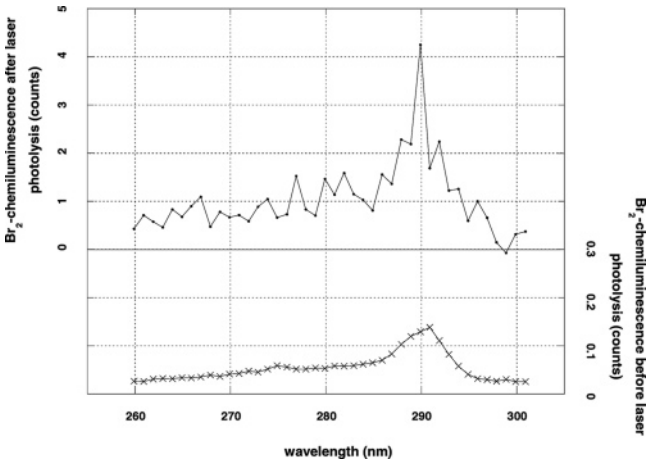


**Figure 8.** Background-corrected ultraviolet chemiluminescence spectrum (● trace) obtained 300 $\mu$s after 248-nm laser photolysis of $CHBr_3$ in excess O atoms produced in a $N_2O$ microwave discharge, with $O_2$ ($1.0 \times 10^{15}$ molecule $cm^{-3}$) and $CH_4$ ($5.0 \times 10^{15}$ molecule $cm^{-3}$) present in 2.0 Torr He at 298 K. The × trace spectrum is obtained when the laser is off. The strong $Br_2$ (D→A) electronic emission at ~289.9 nm is clearly identified. Continuous emissions at shorter wavelengths with possibly weaker diffuse band(s) can also be discerned. The data have not been normalized for any variation in the photon detection efficiency of our photomultiplier over this wavelength region.

of consumption of the $CH(a^4\Sigma^-)$, whereas the methane served to rapidly remove the $CH(X^2\Pi)$ through its fast reaction with it and reduce the Cameron band fluorescence quantum yield by quenching the CO(a) produced in these reactions. The long delay time further served to reduce the detection yield of the CO(a) and OH(A) products relative to Z* produced in the photolysis. Since the signal level for the slowly decaying Z* chemiluminescence is less than ~5% of the fast decaying components (see Figure 7), the spectral data this time was recorded in steps of 1 nm, and at each spectrometer setting, the signal between 300 and 1000 $\mu$s was integrated and co-added for 10 000 laser flashes to improve the signal-to-noise ratio of the data. Figure 8 shows the result. The × trace is the pretrigger background spectrum obtained before the laser fires. The ● trace is the background subtracted spectrum obtained in the photolysis run. The apparent noise in the data set between each spectrometer setting is probably statistical in nature as a result of integrating the weakly decaying chemiluminescence signal in the photolysis. Nevertheless, a pronounced feature at ~289.9 nm for the Z* species is seen. Weaker continuous emissions at shorter wavelengths with possibly diffuse bands are also discernible. This spectrum clearly shows that, when a spectrometer setting of 282.2 nm is chosen to study the OH(A) chemiluminescence as in Figure 7, there will be a phenomenological curvature in the trace because of the simultaneous detection of the Z* radiation. Note that similar result for both the background (no photolysis) and in the photolysis runs were also observed earlier in Figure 3 when $CBr_4$ was used instead of $CHBr_3$ under excess O-atom conditions. This suggests that in both cases the photolysis in excess O atoms yields the same precursor, Y, which reacts further with the O atoms to yield Z*. Furthermore, the species Y, is also generated in the absence of any photolysis when $CBr_4$[37] or $CHBr_3$ is oxidized in excess O atoms. We identify the observed strong feature at ~289.9 nm to be the $Br_2$ (D→A) electronic transition in the (0→0) band[21] with the weaker, short-wavelength diffuse features associated with emissions possibly (from other nearby states) to the ground-electronic state. The intensity of this chemiluminescence signal had a (1.30 ± 0.26) dependence on the laser fluence employed. This suggests that the Y precursor is formed

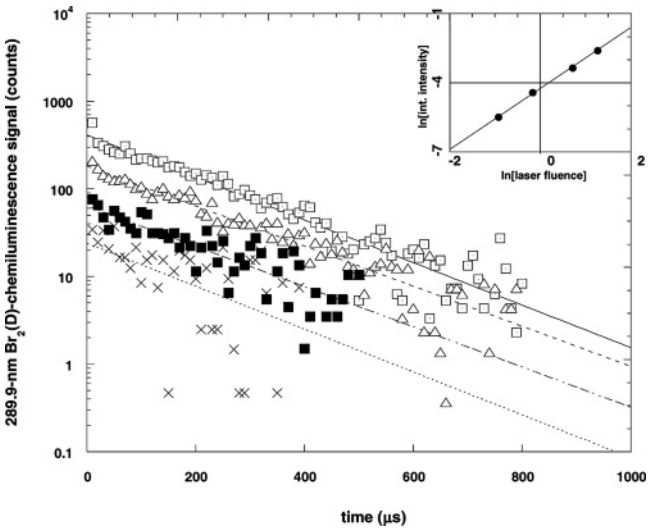


**Figure 9.** Time-resolved 289.9-nm $Br_2$(D) chemiluminescence traces obtained in the photolysis of $CHBr_3$ ($7.0 \times 10^{12}$ molecule $cm^{-3}$) at four different 248-nm laser fluences. The O atoms ($9.0 \times 10^{13}$ molecule $cm^{-3}$) were generated by discharging $N_2O$ ($2.2 \times 10^{14}$ molecule $cm^{-3}$) in a microwave cavity. The data were recorded in the presence of excess $CH_4$ ($5.0 \times 10^{15}$ molecule $cm^{-3}$) in 2.0 Torr He at 298 K. The $CH_4$ helps to minimize the detection of any OH(A) emissions in the red wing of its (1→0) band and any CO(a) emissions such as in the (6→12) band at this wavelength, since it (1) rapidly scavenges any $O(^1D)$ formation from $N_2O$ photolysis and thus minimizes $O_2$ formation, (2) rapidly removes the $CH(X^2\Pi)$ formed in $CHBr_3$ photolysis, and (3) efficiently quenches the CO(a) fluorescence signal. The lines are exponential fits to the data set. The inset shows the plot of the logarithmic of the integrated intensity (i.e., the area) of these curves as a function of the logarithmic of the laser fluence used.

in the detection zone through a 1-photon absorption process. Figure 9 shows the fluence dependence of the 289.9-nm signal. A study of the decay kinetics of the 289.9-nm chemiluminescence in excess $CH_4$ in varying amounts of molecular oxygen and O atom was performed to yield second-order reaction rate coefficient values of $<9 \times 10^{-14}$ and $(5.4 \pm 1.0) \times 10^{-11}$ $cm^3$ $molecule^{-1}$ $s^{-1}$ in 2.0 Torr He and at 298 K for the reaction of the precursor Y with $O_2$ and O atoms, respectively. The Y + $CH_4$ reaction rate coefficient was again estimated to be $<7 \times 10^{-14}$ $cm^3$ $molecule^{-1}$ $s^{-1}$. It is to be noted that these values are similar to the ones obtained when the slowly decaying 282.2-nm chemiluminescence of Figure 7 was analyzed. Since the production of $Br_2$(D) in the fast O-atom reaction requires the precursor Y to have at least 2 bromine atoms in its molecular formula, we interpret our above kinetics data as that for Y being the $CBr_2$ species. Note that the O-atom reactions with $CHBr_2$* and with $CBr_3$* (if directly formed in $CHBr_3$ photolysis) are both endothermic for the production of $Br_2$(D). There are no literature data available for comparison; however, our measured rate coefficients for $CBr_2$ are consistent with the trends exhibited by its homologous counterparts.[41]

**3.5. Reaction Mechanisms.** *3.5.1. Production of $CBr_2$ and $Br_2$(D).* The $Br_2$(D→A) emissions seen in our "cold" $CHBr_3$/O-atom flame in the absence of any photolysis (× trace of Figure 8) can be rationalized by the following sequence of reactions in excess O atoms:[2,23]

| | $\Delta H^o_{298K}$ (kcal $mol^{-1}$) | |
|---|---|---|
| $CHBr_3 + O \rightarrow OH + CBr_3$ | (−8.3) | (13) |
| $CBr_3 + O \rightarrow CBr_2 + BrO$ | (−0.2) | (14) |
| $CBr_2 + O \rightarrow CO + Br_2$ | (−156.0) | (15) |

The bromoform undergoes slow oxidation principally via the H-abstraction reaction 13.[37] The tribromomethyl radical product undergoes facile oxidation by the O atoms, which in its Br-abstraction reaction channel 14 yields the dibromomethylene radical. This then rapidly reacts with the O atoms, and in the very exothermic reaction channel 15, molecular elimination takes place to give ($CO + Br_2$). There is sufficient reaction enthalpy available in this process to electronically excite the bromine molecule up to the D state. The $Br_2(D)$ has a reported radiative lifetime of ~10 ns[42] and is known to relax principally via the (D→A) electronic emission near 289.9 nm. Electronically excited carbon monoxide up to the a-state can also form in this reaction. Evidence for this is provided elsewhere,[37] where we report very weak CO(a) chemiluminescence spectra in the 180−260 nm range for $CHBr_3$/O atom and $CBr_4$/O atom cold flames. It is argued that in these cold flames CBr production will be negligible (relative to $CBr_2$), and therefore, the ($CBr + O \rightarrow Br + CO(a)$) reaction does not play a major role in the production of the observed CO(a) chemiluminescence. Also, since CH formation should not be possible in the $CHBr_3$/O atom flame, the ($CH + O \rightarrow H + CO(a)$) reaction cannot be used here to explain these emissions.

The fast rise in the $Br_2(A)$ signal in Figure 9 suggests that when a $CHBr_3$/O-atom mixture is photolyzed, there is photolytic production of $CBr_2$. However, previous work[17,18] had failed to detect any dibromomethylene formation in $CHBr_3$ photodissociation. Therefore, Figure 9 provides first evidence that perhaps a very small fraction of the photolysis may indeed be proceeding via the ($CHBr_3 + h\nu \rightarrow CBr_2 + HBr$) channel 12 to directly yield $CBr_2$. Furthermore, the data of Figure 9 also reveals that the rate of decay of the chemiluminescence is not quite exponential; that is, the initial decay rate is somewhat suppressed. Therefore, a second photochemical source for $CBr_2$ formation may also be operative. A possible route for this would be the ($CHBr_2 + O \rightarrow CBr_2 + OH$) reaction, where the dibromomethyl radical is produced in the initial photolysis of the $CHBr_3$. Furthermore, since the $CBr_3$ radical, formed in reaction 13, will also be present in the detection zone, its photolysis ($CBr_3 + h\nu \rightarrow CBr_2 + Br$) may generate more $CBr_2$. The relative importance for these three processes has not been ascertained in this work; however, from the huge signal in the upper trace of Figure 8 relative to that of the lower trace, it can be shown that the first two sources discussed above should dominate. In any case, the observed linear dependence of the 289.9-nm chemiluminescence intensity on the fluence of the photolysis laser is consistent with the production of $CBr_2$ via any combination of the above three photolytic mechanisms. It also implies that 2-photon absorption processes to generate $CBr_2$ via $CHBr_3 + h\nu \rightarrow CHBr_2 + Br$ (reaction 5), followed by $CHBr_2 + h\nu \rightarrow CBr_2 + H$; or $CHBr_3 + h\nu \rightarrow CBr_3 + H$, followed by $CBr_3 + h\nu \rightarrow CBr_2 + Br$ are relatively unimportant compared to the above mechanisms. This further suggests that the primary quantum yields for $CBr_3$ and $CBr_2$ production, respectively, in 1-photon photolysis of $CHBr_3$[43] and $CHBr_2$[18] are very small, and therefore H-atom production must also be negligible.

*3.5.2. Production of CO(A and a) and CH(X and a).* Our measured CO(A) chemiluminescence decay trends with various added substrates indicate that the prominent source for CO(A) is the $CH(a^4\Sigma^-) + O$ reaction when excess $CH_4$ is present in the photolysis mixture. The 2-photon generation of the quartet methylidyne radical can be summarized as the process: $CHBr_3 + 2h\nu(248\ nm) \rightarrow CH(a^4\Sigma^-) + Br_2 + Br$; $\Delta H^o_{298K} = \sim -43.0$ kcal mol$^{-1}$. On removing the methane, there is an enhancement in the CO(A) signal by ~4 times; however, the chemiluminescence decay is no longer exponential. This is because the doublet methylidyne radical also formed in the photolysis: $CHBr_3 + 2h\nu(248\ nm) \rightarrow CH(X^2\Pi) + Br + Br_2$ (or $Br + Br$); $\Delta H^o_{298K} = \sim -60.5$ (or $\sim -14.5$) kcal mol$^{-1}$ is now available to participate in the O-atom reaction. In this case, the production of CO(A) can only be possible if the doublet methylidyne radical processes at least 9.2 kcal mol$^{-1}$ of internal energy. Since any rotationally excited doublet methylidyne will rapidly thermalize in the 2 Torr He buffer gas, the presence of vibrationally excited species such as $CH(X^2\Pi, v'' \geq 2)$ is necessary to explain the top trace in Figure 2. Previously[44] it has been shown that both the $v'' = 1$ and $v'' = 2$ vibrational states are not efficiently quenched by helium. It can be shown that in the present experiments the reactions of O atoms and that of any added substrate will compete with the slow quenching by the He in the removal of these species. The areas of the traces in Figure 2 only provide values for the phenomenological source strengths for CO(A) chemiluminescence, since information on the integrated yield of $CH(a^4\Sigma^-, v' \geq 0)$ relative to $CH(X^2\Pi, v'' \geq 2)$ is not available in the 2-photon, 248-nm dissociation of $CHBr_3$, nor is there data available on the state-specific branching fractions for the production of CO(A) in their reactions with the O atoms. The (CH(a) + O) and (CH(X) + O) source strengths are deduced to be ~25% and ~75%, respectively. As there is pronounced phenomenological curvature in the top trace of Figure 2, we did not attempt to measure the second-order rate coefficients for the initial decay of the chemiluminescence in the added substrates NO and $O_2$ since such an analysis would under estimate the true value of their reaction rate coefficients with $CH(X^2\Pi, v'' \geq 2)$. For the $N_2O$, $H_2$, and $CH_4$ substrates, the initial decay rate depended linearly on the substrate concentrate and gave second-order rate coefficients values that were consistent with previous measurements.[10,28]

The overall bimolecular rate coefficients of O-atom reactions with $CH(X^2\Pi)$ and $CH(a^4\Sigma^-)$ are very large and similar in value. Formation of ground-state ($CO(X^1\Sigma^+) + H(^2S)$) products (or ($CO(A^1\Pi) + H(^2S)$) in the system is spin allowed and expected to proceed via an addition/elimination reaction mechanism on a doublet potential energy surface. Formation of the ($CO(a^3\Pi + H(^2S)$) products could proceed via a doublet and/or a quartet potential energy surface. The lifetime of the energized intermediate(s), {HCO}*, will be very short of the order of a vibrational period. If dissociation directly produces CO in any of the energetically allowed states, the corresponding ultraviolet chemiluminescence signals in the reaction will have growth maxima that will be determined by the experimental lifetime, $\tau$, of the emitting products. The distinct rise in the (top) ● trace of Figure 2 for the 165.7-nm chemiluminescence signal associated with the $CO(A^1\Pi, v' = 0)$ emitter, whose radiative lifetime is known to ~10 ns, suggests that this product does not exclusively form directly from the energized {HCO}* intermediate. This was confirmed by recording the 165.7-nm CO(A) chemiluminescence trace with a higher time resolution of 2 $\mu$s where a large instantaneous signal followed by a small rise that typically maximized at ~10 $\mu$s was observed. This implies that, in addition, there are a set of other CO states that are the initial products from {HCO}* dissociation which then undergo very fast intersystem crossing to yield $CO(A^1\Pi)$. Most likely these are the $(a^3\Pi)$ meta-stable states near $v' = 11$ that cross over to the $(A^1\Pi)$ vibrational manifold through collisions with excess O atoms/$O_2$ (and buffer gas[45]) via near-resonant energy transfer processes, see Figure 10. The nearby vibrational manifold of the $(a'^3\Sigma^+)$ and $(d^3\Delta)$ states could also populate the $A(^1\Pi)$

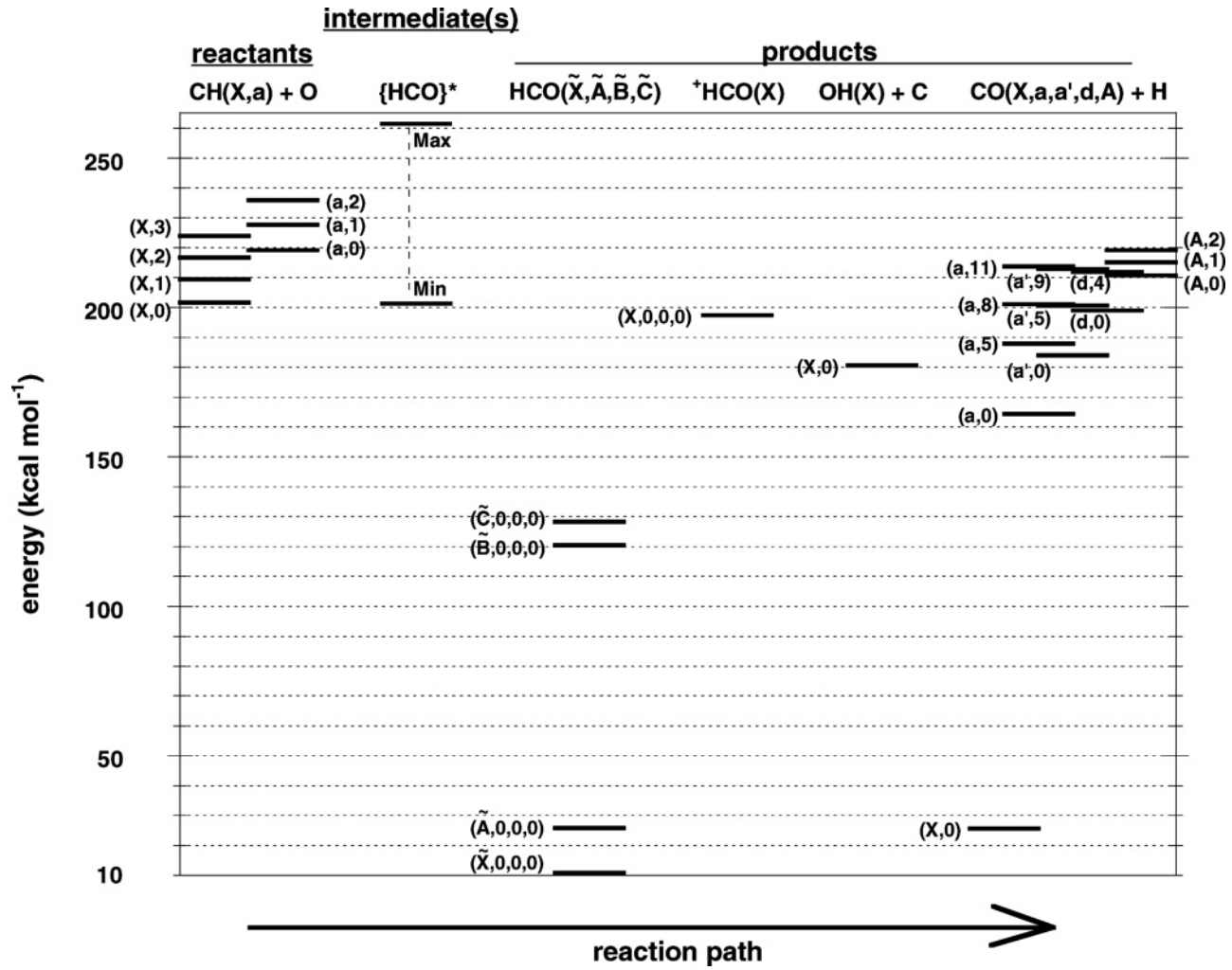


**Figure 10.** Schematic energy diagram for the (CH + O) reaction system. The labels refer to the electronic and the vibrational levels of the radical species. Only those levels relevant to the present discussion are shown. The energy range of the intermediate is indicated by the min/max limits possible as a result of 2-photon 248-nm dissociation of $CHBr_3$.

system through spin−orbit and rotation−electronic interactions. However, these states have high Einstein transition probabilities for spontaneous decay to the lower vibrational levels of the ($a^3\Pi$) state and therefore should principally decay via visible-ir emissions, with radiative lifetimes in the few microsecond range. Future high-level ab initio theoretical calculations on the (CH + O → CO + H) system should offer further insight about the potential energy surface(s), the transition state(s), the reaction intermediate(s), and the reaction dynamics involved. It is to be noted that in the related ($CH + O_2 \rightarrow CO + OH$) reaction, the initial energized reaction adduct, {OOCH}*, undergoes fast rearrangement/dissociation via a four-center intermediate to directly yield the OH(A) product since no rise in the 282.2-nm signal is seen in the × trace of Figure 7.

Hydrocarbon flame emissions due to electronically excited formyl radicals could not be positively identified in the photolysis. The (0,0,0 → 0,0,0) band origins for the ($\tilde{B}\rightarrow\tilde{X}$) and ($\tilde{C}\rightarrow\tilde{X}$) transitions are near 258.2 and 241.3 nm, and therefore lie within the strong CO(a→X) Cameron band emissions. Our 220−280 nm spectral scans of the chemiluminescence in $CHBr_3$/O atom photolysis were very similar to those obtained in $CBr_4$/O atom photolysis in which HCO($\tilde{B}$ or $\tilde{C}$) cannot form. In both cases, all the observed vibronic peaks could be assigned to CO(a→X) transitions.[37] Therefore, in the present experiments, the {HCO}* intermediate cannot be stabilized efficiently to yield any significant amounts of electronically excited formyl radicals.

*3.5.3. Check for CH($a^4\Sigma^-$) → CH($X^2\Pi$) Collisional Processes.* In the above discussions, the phenomenological curvatures in the ● trace of Figure 2 and in the × trace of Figure 7 were explained by suggesting that reactions of both CH($X^2\Pi$) and CH($a^4\Sigma^-$) independently contribute to the production of the excited products, CO(A) and OH(A), respectively. However, an alternate mechanism needs to be considered in which the CH($a^4\Sigma^-$) does not directly produce any excited products in its reactions, but rather slowly generates more CH($X^2\Pi$) in the system after the photolytic pulse. Through collisions with excess buffer gas it could well be that the CH($a^4\Sigma^-$, $v' = 0$) undergoes intersystems crossing to produce CH($X^2\Pi$, $v'' \leq 2$). In this case, the [CH(X)] temporal profile would be of the form: $[CH(X)]_0 e^{-k_{CH(x)}.t} + k_{He}[He][CH(a)]_0(e^{-k_{CH(a)}.t} - e^{-k_{CH(x)}.t})/(k_{CH(x)} - k_{CH(a)})$, where $[CH(X)]_0$ and $[CH(a)]_0$ respectively are the initial photolytic yields of the doublet and quartet methylidyne radicals, with $k_{CH(x)}$ and $k_{CH(a)}$ as their corresponding pseudo-first-order decay coefficients, and $k_{He}$ as the second-order rate coefficient for He collisions with CH(a) that lead to CH(X) production. This type of a [CH(X)] temporal profile will also lead to nonexponential chemiluminescence decay signals for the excited-state species formed in CH(X) reactions, and in excess [$CH_4$] conditions, the decay rate of the remaining chemiluminescence signal will provide a measure of the

reactivity of CH(a) with any added substrate. If this alternate scheme predominates in our photolysis, both the chemiluminescence yield and its decay rate will be dependent on the He pressure. To test for this, the related reaction of NO with methylidyne radicals was studied in $5 \times 10^{15}$ molecule $cm^{-3}$ of $CH_4$ at two different He pressures of 2.0 and 22.0 Torr. The 336.2-nm emission from the $NH(A^3\Pi)$ product[46] was monitored at constant [NO], [$CHBr_3$], and laser fluence conditions. The higher pressure experiment produced no enhancement in the chemiluminescence signal. An upper limit of $k_{He} < 1 \times 10^{-14}$ $cm^3$ $molecule^{-1}$ $s^{-1}$ was estimated for the reaction rate coefficient for removal of CH(a) by He. These results imply that the imidogen radical can also directly form in the (CH(a) + NO) reaction through a short-lived four-center reaction intermediate and that the conversion of CH(a) to CH(X) in the present work plays a minor role in producing the observed nonexponential chemiluminescence decay traces. The $k_{NO}$ rate coefficients for (CH(X) + NO) and (CH(a) + NO) reactions were also determined from the decays of the 336.2-nm traces. At 298 K, the $k_{NO}$ values were respectively $(1.8 \pm 0.3) \times 10^{-10}$ and $(4.2 \pm 0.7) \times 10^{-11}$ $cm^3$ $molecule^{-1}$ $s^{-1}$, and were shown to be independent of the He pressure employed. These values are consistent with previous literature numbers.[28,46,47]

## 4. Conclusions

Strong ultraviolet chemiluminescence was observed in the laser photolysis of $CHBr_3$/O atom/$O_2$ mixtures in 2 Torr of He. Spectral scans in the 120−300 nm wavelength range showed CO(A), CO(a), $Br_2$(D), and OH(A) to be the prominent emitters. The photoproducts of $CHBr_3$ photolysis react with O atoms to generate CO(A), CO(a), and $Br_2$(D) and react with $O_2$ to generate OH(A). The identities of these photoproducts were established by studying the laser fluence dependence of the chemiluminescent intensities, by carrying out kinetic trend analysis on how the chemiluminescent decay behaved in various added substrates, and by making comparisons of the observed second-order rate coefficient data to literature values. The methylidyne radicals $CH(X^2\Pi)$ and $CH(a^4\Sigma^-)$ were thereby identified to be involved in the production of CO(A), CO(a), and OH(A) and the dibromomethylene radical ($CBr_2$) in the production of $Br_2$(D). The present work provides evidence for the first time that supports the idea that the interaction of thermospheric O atoms with carbonaceous species such as CH of the Space Shuttle plumes could be responsible for part of the far-field ultraviolet emissions observed there.[13]

**Acknowledgment.** Funding for this work was provided by the Air Force Office of Scientific Research under Contract No. F04611-99-C-0025 with the Air Force Research Laboratory, Edwards AFB, CA 93524.

## References and Notes

(1) Baulch, D. L.; Cobos, C. J.; Cox, R. A.; Esser, C.; Frank, P.; Just, Th.; Kerr, J. A.; Pilling, M. J.; Troe, J.; Walker, R. W.; Warnatz, J. *J. Phys. Chem. Ref. Data* **1992**, *21*, 411.

(2) DeMore, W. B.; Sander, S. P.; Howard, C. J.; Ravishankara, A. R.; Golden, D. M.; Kolb, C. E.; Hampton, R. F.; Kurylo, M. J.; Molina, M. J. *Chemical Kinetics and Photochemical Data for Use in Stratospheric Modeling;* Evaluation No. 12, JPL Publication No. 97-4; Jet Propulsion Laboratory: Pasadena, CA, 1997.

(3) NIST chemistry webbook, http:/webbook.nist.gov.

(4) Messing, I.; Filseth, S. V.; Sadowski, C. M.; Carrington, T. *J. Chem. Phys.* **1981**, *74*, 3874.

(5) Calcote, H. F. *8th Symposium (International) on Combustion*; Williams & Williams: Philadelphia, 1962; p 184.

(6) Vinckier, C. *J. Chem. Phys*. **1979**, *83*, 1234.

(7) Peeters, J.; Vinckier, C. *15th Symposium (International) on Combustion*; The Combustion Institute: Pittsburgh, 1975; p 969.

(8) Murrell, J. N.; Rodriguez, J. A. *J. Mol. Struct. Theochem.* **1986**, *139*, 267.

(9) Lin, M. L. *Int. J. Chem. Kinet.* **1974**, *6*, 1.

(10) Vaghjiani, G. L. *J. Chem. Phys.* **2003**, *119*, 5388.

(11) Phippen, D. E.; Bayes, K. D. *Chem. Phys. Lett*. **1989**, *164*, 625.

(12) Cool, T. A.; Tjossem, P. J. H. *Chem. Phys. Lett.* **1984**, *111*, 82.

(13) Viereck, R. A.; Murad, E.; Knecht, D. J.; Pike, C. P.; Bernstein, L. S.; Eglin, J. B.; Broadfoot, A. L. *J. Geophys. Res*. **1996**, *A101*, 5371.

(14) Vaghjiani, G. L. *J. Phys. Chem.* **2001**, *A105*, 4682.

(15) Vaghjiani, G. L.; Ravishankara, A. R. *J. Phys. Chem*. **1989**, *93*, 1948.

(16) Bayes, K. D.; Toohey, D. W.; Friedl, R. R.; Sander, S. R. *J. Geophys. Res*. **2003**, *D108*, 4095.

(17) Xu, D.; Francisco, J. S.; Huang, J.; Jackson, W. M. *J. Chem. Phys.* **2002**, *117*, 2578.

(18) Zou, P.; Shu, J.; Sears, T. J.; Hall, G. E.; North, S. W. *J. Phys. Chem*. **2004**, *A108*, 1482.

(19) Lindner, J.; Ermisch, K.; Wilhelm, R. *Chem. Phys*. **1998**, *238*, 329.

(20) Chang, B.-C.; Guss, J.; Sears, T. J. *J. Mol. Spectrosc.* **2003**, *219*, 136.

(21) Huber, K. P.; Herzberg, G. *Molecular Spectra, Molecular Structure: IV Constants of Diatomic Molecules*; Van Nostrand Reinhold Company: New York, 1979.

(22) Born, M.; Ingemann, S.; Nibbering, N. M. M. *J. Am. Chem. Soc.* **1994**, *116*, 7210.

(23) Born, M.; Ingemann, S.; Nibbering, N. M. M. *Int. J. Mass. Spectrom. Chem*. **2000**, *194*, 103.

(24) Dixon, D. A.; de Jong, W. A.; Peterson, K. A.; Francisco, J. S. *J. Phys. Chem.* **2002**, *A106*, 4725.

(25) Schwartz, M.; Marshall, P. *J. Phys. Chem.* **1999**, *A103*, 7900.

(26) Okada, S.; Yamasaki, K.; Matsui, H.; Saito, K.; Okada, K. *Bull. Chem. Soc. Jpn.* **1993**, *66*, 1004.

(27) Mehlmann, C.; Frost, M. J.; Heard, D. E.; Orr, B. J.; Nelson, P. F. *J. Chem. Soc., Faraday Trans*. **1996**, *92*, 2335.

(28) Hou, Z.; Bayes, K. D. *J. Phys. Chem*. **1993**, *97*, 1896.

(29) Husain, D.; Kirsch, L. J. *Trans. Faraday Soc*. **1971**, *67*, 2025.

(30) Husain, D.; Young, A. N. *J. Chem. Soc., Faraday Trans. 2* **1975**, *71*, 525.

(31) Dorthe, G.; Caubet, Ph.; Vias, Th.; Barrere, B.; Marchais, J. *J. Phys. Chem.* **1991**, *95*, 5109.

(32) Liu, W.-L.; Chang, B.-C. *J. Chin. Chem. Soc.-Taip*. **2001**, *48*, 613.

(33) Chang, B.-C.; Sears, T. J. *J. Chem. Phys.* **1996**, *105*, 2135.

(34) Xu, S.; Beran, K. A.; Harmony, M. D. *J. Phys. Chem.* **1994**, *98*, 2742.

(35) Dornhofer, G.; Hack, W. *J. Chem. Soc., Faraday Trans. 2* **1988**, *84*, 441 and references therein.

(36) Wagner, R.; Wagner, H. Gg. *Z. Phys. Chem*. **1992**, *175*, 9.

(37) Vaghjiani, G. L. *Chem. Phys. Lett*. Work to be published.

(38) McDaniel, R. S.; Dickson, R.; James, F. C.; Strausz, O. P. *Chem. Phys. Lett*. **1976**, *43*, 130.

(39) Marr, A. J.; Sears, T. J.; Davies, P. B. *J. Mol. Spectrosc.* **1997**, *184*, 413.

(40) Vaghjiani, G. L. *J. Chem. Phys*. **1996**, *104*, 5479.

(41) *17. NIST Chemical Kinetics Database: Version 2Q98*; Standard Reference Data Program; National Institute of Standards and Technology: Gaithersburg, MD 1998; references therein.

(42) Austin, D. I.; Donovan, R. J.; Hopkirk, A.; Lawley, K. P.; Shaw, D.; Yencha, A. J. *Chem. Phys*. **1987**, *118*, 91.

(43) McKee, K.; Blitz, M. A.; Hughes, K. J.; Pilling, M. J.; Qian, H.-B.; Taylor, A.; Seakins, P. W. *J. Phys. Chem*. **2003**, *A107*, 5710.

(44) Blitz, M. A.; Pesa, M.; Pilling, M. J.; Seakins, P. W. *Chem. Phys. Lett*. **2000**, *322*, 280.

(45) Kittrell, C.; Cameron, S.; Butler, L.; Field, R. W. *J. Chem. Phys.* **1983**, *78*, 3623.

(46) Lichtin, D. A.; Berman, M. R.; Lin, M. C. *Chem. Phys. Lett.* **1984**, *108*, 18.

(47) Bergeat, A.; Calvo, T.; Daugey, N.; Loison, J. C.; Dorthe, G. *J. Phys. Chem*. **1998**, *A102*, 8124.